TECHNICAL RESEARCH REPORT

SYSTEMS RESEARCH CENTER

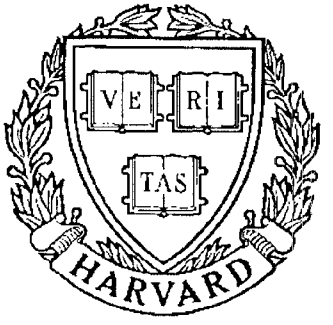

Supported by the National Science Foundation Engineering Research Center Program (NSFD CD 8803012), Industry and the University

Dynamic Generation of Machined Surfaces Part 2: Construction of Surface Topography

by G.M. Zhang and S.G. Kapoor

TR 90-37

Dynamic Generation of Machined Surfaces Part 2: Construction of Surface Topography

G. M. Zhang, Assistant Professor
Mechanical Engineering Department and Systems Research Center
University of Maryland
College Park, MD 20742

S. G. Kapoor, Associate Professor
Department of Mechanical and Industrial Engineering
University of Illinois at Urbana-Champaign
Urbana, Illinois 61801

Abstract

In Part 1 of these two-part papers, a normal distribution model has been formulated to describe the random excitation system present during machining. Part 2 presents a methodology to dynamically generate the surface topography under the random excitation environment through computer simulation. The proposed methodology uses the tool vibratory motion along with the tool geometrical motion to construct the topography of a machined surface. Both experimental and simulation results confirm that when a small feed is used, the influence of the spiral trajectory of tool geometrical motion on the surface generation decays dramatically and the random excitation system, on the opposite, is strengthened playing a significant role in surface texture generation.

1 Introduction

Machined surface topography observed after machining with a single-point tool originates from two parts of the tool motion. The first part is the tool geometrical motion and the second part is the tool vibration about its dynamic equilibrium position.

The tool geometrical motion is deterministic in nature. Under a turning or boring machining operation, the motion can be described as a spiral trajectory in space shown in Fig. 1a. In this simulation, the tool nose radius is assumed to be 0.80 mm and there is no tool vibratory motion. The three dimensions in Fig. 1a represent the directions related to feed, cutting speed, and depth of cut. Note that the cross-sectional view along the feed

direction presents a typical surface profile of machined surfaces.

The tool vibratory motion, as discussed in Part 1 [1], is random in nature. If we assume that the tool vibratory motion takes the form of $3sin50t$ (μm) about its dynamic equilibrium position during machining, the tool vibratory motion when integrated with the tool geometrical motion will lead to formation of the surface topography as shown in Fig. 1b. Comparing these two surface topographies, Fig. 1b looks like surfaces normally observed in practice. This indicates that the tool vibratory motion can play an important role in the dynamic generation of surface topography.

Most research work in the area of vibration control focuses on studying the closed chatter loop and the regenerative feedback path of machining system [2,3]. The feedback path transmits the surface modulations produced by the tool vibratory motion from one revolution to the next. However, if the regenerative process is convergent, which is equivalent to say that the closed chatter loop is stable in the sense of Lyapunov [4], the tool vibratory motion during machining will be gradually attenuated and finally vanish due to the damping effect present in the machining process. Under such circumstances, the generation of surface topography would be eventually dominated by the tool cutting geometrical motion to produce surface topographies similar to that indicated in Fig. 1a. Unfortunately, it has been observed in practice that the tool vibratory motion during a stable machining process never vanishes, but stays at an almost constant level because of the presence of a random excitation system during machining.

The significance of these two-part papers is to develop a methodology which takes into account both the random excitation system and the tool geometrical motion for the dynamic generation of three-dimensional texture of machined surfaces. In this paper, the basic methodology for surface topography construction is presented in Section 2. For the purpose of simulating the system response, i.e., the tool vibratory motion during machining, a boring machining system model is used. Section 3 shows how the random excitation system formulated in Part 1 can be used as an input to the machining system model. Section

4 describes the development of two parametric tool path equations which quantitatively determine the coordinates of surface profiles generated during machining. In Section 5, the tool vibratory motion is integrated with the parametric tool path equations leading to the dynamic generation of surface topography. Section 6 discusses the simulation and experimental results and provides an insight about the effect of the cutting parameter feed on the surface texture generation.

2 Surface Generation Methodology

Figure 2 is a block diagram illustrating the basic methodology developed in the present work to study the mechanism of the dynamic generation of machined surface topographies. The methodology uses the tool vibratory response and the spiral trajectory of tool geometrical motion to generate the surface topography. A machining system model is employed to manipulate the tool vibratory response due to input functions such as nominal chip load, random excitation function representing the nonhomogeneity of material hardness and the residual chip load from the regenerative mechanism. The spiral trajectory is computed based on the tool geometry and the feedrate. Finally, the parametric tool path equations are developed by integrating the tool geometrical trajectory with the appropriate tool vibratory response to generate the three-dimensional surface topography.

The simulation strategy is built upon four modules, i.e., the input function module, the system model module, the tool geometrical motion module, and the topography generation module in which a three-dimensional graphics package is included. The descriptions of these modules are given below.

2.1 Input Function Module

As shown in Fig. 2, the input module is made up of three input functions. The first input function is a step function. Its magnitude represents the nominal chip load. The jump discontinuity, which is set to $time = 0$, indicates the beginning of machining operation.

This step function representation resembles situations on the shop floor where an operator selects the depth of cut and feed when the machining operation begins. The second input function represents the residual chip load, a concept proposed in [5,6]. Due to the tool vibratory motion, the generation of surface modulations during machining is unavoidable, and the modulations generated during the first revolution of the workpiece will be added to, or subtracted from, the nominal chip load during the second revolution of the workpiece. Such a transmission process continues along with the cutting process. As indicated in Fig. 2, there is a multiplication (overlap) factor μ in the representation of the second input function. This multiplication factor reflects the overlapping of the cutting area between the two successive revolutions of the workpiece. For example, the multiplication factor is equal to unity for plunge cutting, and is equal to zero for thread cutting (indicating there is no residual chip load during machining). The third input function is a statistical function representing the random excitation system present during machining. The origination of this random excitation system is due to the existence of a nonhomogeneous distribution of microhardness present in the workpiece material being cut. The statistical function is assumed to be a normal distribution [1]. The incorporation of this normal distribution as an input function to the system module requires it to be in a format compatible with the other two input functions, and will be discussed in detail in Section 3.

2.2 System Model Module

The system model module is designed to simulate the response of the machining system, i.e., the tool vibratory motion during machining when subjected to the three input functions discussed in Section 2.1. In the present work, a boring machining system model is chosen for the simulation of tool vibratory motion due to the simplicity and explicitly of its model representation. The chosen model, which was formulated in the state variable space [6], has the following matrix form.

$$[\dot{x}_1(t)\ \dot{x}_2(t)\ \dot{x}_3(t)\ \dot{x}_4(t)]^T = [A][x_1(t)\ x_2(t)\ x_3(t)\ x_4(t)]^T + [B]u(t) \qquad (1)$$

$$y(t) = [C][x_1(t)\ x_2(t)\ x_3(t)\ x_4(t)]^T$$

where $[x_1(t)\ x_2(t)\ x_3(t)\ x_4(t)]^T$ is the state vector representing the displacements and velocities of the two principal modes of the boring system as indicated in Fig. 3. Matrices $[A]$, $[B]$, and $[C]$ are related to characteristics of the cutting process and the boring bar structure such as the diameter and length of the boring bar, the bar material, and the cross-section geometry, $u(t)$ is a scalar function representing the input to the boring system model, and $y(t)$ is the system response representing the tool motion in the direction perpendicular to the machined surface.

The scalar function $u(t)$ is equal to a sum of the three input functions. In order to sum them up, from the simulation standpoint, the second input function (residual chip load) is modified in such a way that it takes the form of a rectangular wave function. This modification can be regarded as digitizing the surface modulations produced during machining in a uniform time interval ΔT. For example, if the spindle rotatory speed is assumed to be N rpm, so that the time needed for one revolution of the workpiece during machining is $60/N$ sec, the uniform time interval, or sampling interval ΔT is given by

$$\Delta T = \frac{60}{N * n_s} \tag{2}$$

where n_s = number of samples taken along the circumference of workpiece during one revolution of the workpiece, and

N = spindle speed, rpm.

Such a modification not only simplifies the summation of the first two input functions, but also sets up the time interval base for summing up the third input function and the basic time interval used in the simulation process.

2.3 Tool Geometrical Motion and Topography Generation Modules

The tool geometrical motion module considers the effect of tool spiral motion, determined by the workpiece rotation and tool feed motion, on the generation of surface topography.

There is also an interaction between the tool geometrical motion and the tool vibratory motion. Section 4 presents a discussion on this module with focus on the determination of two parametric tool path equations.

The topography generation module in Fig. 2 integrates the tool vibratory motion (output of module 2) with the tool geometrical motion (output of module 3). This module generates a numerical data base for constructing a three-dimensional surface topography. Section 5 presents a five-step procedure for the dynamic generation of a machined surface.

3 Incorporation of the Random Excitation System as an Input Function

The third input function is a statistical function representing the random excitation system. The unit of this normal distribution function is Brinell Hardness Number (BHN) [1]. Therefore, a procedure to convert the unit of BHN to the unit of mm^2 for consistency with the first two input functions is needed.

3.1 Relation between Cutting Force and Material Hardness

The scientific basis for developing this procedure is the theory proposed by Kronenberg to establish the relation between the cutting force and hardness of workpiece material [7]. His formula assumes a direct proportionality between the cutting force and chip load, C_l.

$$Cutting\ Force = K_s * C_l \tag{3}$$

where the proportional coefficient, K_s, is named as the unit cutting force and is related to the hardness of material. The coefficient K_s is usually treated as a constant for evaluating the average cutting force. For evaluation of the instantaneous cutting force to resemble the phenomenon that magnitude of the cutting force jumps up or drops down when the cutting edge meets a hard spot or a soft spot, a ratio term $[\frac{h_i}{\bar{h}}]^m$ is introduced in Eq. (3).

$$Instantaneous\ Cutting\ Force \;=\; K_s * [\frac{h_i}{\bar{h}}]^m * C_l \tag{4}$$

$$for\ i \ = \ 1, 2, \cdots, n_l$$

In Eq. (4), index i represents the i^{th} location on the workpiece during machining, h_i stands for the hardness value at the i^{th} location, $\overline{h}$ is the mean of h_1, $h_2, \cdots, h_{np}$, and n_l represents the hardness mean location. The exponent m is called Meyer exponent to explain the nonlinear relation between the cutting force and the ratio term $\frac{h_i}{\overline{h}}$. The Meyer exponent can be experimentally determined. For example, it has been found that for carbon steel m = 0.454, and for iron and copper m is 0.457 and 0.418, respectively [7].

3.2 Conversion to Equivalent Random Chip Load Variation Form

It is evident that Eq. (4) takes into account the effect of nonhomogeneous nature of material hardness and gives an instantaneous force corresponding to the individual cutting locations. As long as the hardness values at individual cutting locations are known, the dynamic variation of cutting force can be quantitatively evaluated. In this regard, the research work presented in Part 1 is directly applicable for such an evaluation.

It has been shown in Part 1 that the nonhomogeneous distribution of hardness could be characterized by the sample hardness means $(\mu_{s1}, \mu_{s2}, ..., \mu_{sns})$ at individual cutting locations. These sample hardness means obey a normal distribution. The mean of this normal distribution, $\overline{\mu_s}$ or μ_a, represents the mean of all sample hardness means. When applying this normal distribution model to Eq. (4), the following three substitutions can be made to derive Eq. (5).

$$h_i = \mu_{si}, \ \overline{h} = \overline{\mu_s} = \mu_a \quad and \quad n_l = n_s$$

$$Instantaneous\ Cutting\ Force \quad = \quad K_s * [\frac{\mu_{si}}{\mu_a}]^m * C_l \tag{5}$$

Substituting the sample hardness means $(\mu_{s1}, \mu_{s2}, \mu_{s3}...)$at the individual cutting locations in Eq. (5), the instantaneous cutting force can be evaluated. In order to further clarify the effect of the random excitation system on the tool motion during machining, the percentage variation in the nominal chip load, which is due to the nonhomogenous material hardness

distribution, can be separated as follows.

$$Cutting\ Force = K_s * \{ \underbrace{[(\frac{\mu_{si}}{\mu_a})^m - 1]}_{equivalent\ percentage\ variation} + 1\} * C_l \quad (6)$$

The underlined term in Eq. (6) is denoted as the equivalent percentage variation. A product term, i.e., $[(\frac{\mu_s}{\mu_a})^m - 1] * C_l$, is the conversion form of the random excitation system in the unit of mm^2, from the viewpoint of the cutting force generation. In fact, Eq. (6) represents a resultant effect of the first input function (nominal chip load) and the thrid input function (random excitation system) on the cutting force generation.

Following is an example to demonstrate the conversion procedure. Assume that a low carbon steel bar (SAE 1015 and diameter = 50 mm) is being machined under two different cutting parameter settings. The first cutting parameter setting is d=0.50 mm, N=600 rpm, and f=0.25 mm/rev. The second setting is d=0.50 mm, N=600 rpm, and f=0.10 mm/rev. Assume that the microstructural characteristics of this steel bar are shown in Fig. 4 in Part 1 of these two-part papers [1]. The mean μ_a, variance σ_a^2, and the correlation coefficient function $\rho(r)$ as calculated in Part 1 [1] are used to estimate the two random excitation systems under the two cutting parameter settings. Based on Eq. (2) and Eq. (4) in Part 1 [1], the two random excitation systems have the same mean value, $\overline{\mu_{sI}} = \overline{\mu_{sII}} = \mu_a = 126$ (BHN), but different variance values. One is $\sigma_{sI}^2 = 166\ (BHN)^2$ for feed = 0.25 mm/rev. The other is $\sigma_{sII}^2 = 172\ (BHN)^2$ for feed = 0.10 mm/rev. The Meyer exponent is taken to be $m = 0.454$ for low carbon steel. The number of samples is chosen to be $n_s = 33$ based on an assumption that the highest frequency in the cutting force variation is set at $f_{max} = 165\ Hz$, as discussed in Part 1 [1].

The equivalent percentage variation of the nominal chip load for each of these two random excitation systems can be obtained by

1. creating 33 random numbers for sample mean hardness values, μ_{si}, from a normal distribution with $\mu_a = 126$ and $\sigma_{sI}^2 = 166$ or $\sigma_{sII}^2 = 172$.

2. evaluating the equivalent percentage variation by replacing μ_a (the denominator of the term $\frac{\mu_s}{\mu_a}$) by 126 (BHN) and substituting each of the 33 generated random numbers for μ_s in the numerator of the term $\frac{\mu_s}{\mu_a}$ as shown in Eq. (7), i.e.,

$$Equivalent\ Percentage\ Variation\ (EPV) = [(\frac{\mu_{si}}{\mu_a})^m - 1] \qquad (7)$$
$$for\ i\ =\ 1, 2, \cdots, 33$$

The generated sample hardness values and equivalent percentage variations are listed in column 2 and column 3 as well as in column 4 and column 5 of Table 1 for the two random excitation systems. Note that the units listed in column 2 and column 4 are BHN for the two random excitation systems and column 3 and column 5 list their equivalent percentage variations, which are dimensionless. Figure 4 graphically presents the random excitation system ($\mu_a = 126$ and $\sigma_{sI}^2 = 166$) in two equivalent forms. Figure 4a depicts a normal distribution form in terms of the hardness representation and Fig. 4b shows a rectangular wave form which represents the equivalent percentage variation in the nominal chip load. This wave form fluctuates about the nominal chip load, and can be mathematically expressed in a combinational form of step functions as:

$$EPV_{random}(t) = [P_1 s(0) - P_1 s(\Delta T)] + [P_2 s(\Delta T) - P_2 s(2\Delta T)] + \cdots \qquad (8)$$

where P_i = equivalent percentage of the nominal chip load at time $i * \Delta T$,

i = index for the order of samples taken along the circumference of the workpiece,

ΔT = the uniform time interval ($\frac{60}{n_s * N}$), and

$s(i * \Delta T)$ = unit step function with the jump discontinuity at time ($i * \Delta T$).

As indicated in Table 1, the random excitation system plays a role which is equivalent to instantaneously alternate the normal chip load during machining in a range of $\pm 8\%$ ($\sigma_{sI}^2 = 166$ and feed = 0.25 mm/rev) or $\pm 12\%$ ($\sigma_{sII}^2 = 172$ and feed = 0.10 mm/rev). The alternating range associated with feed = 0.10 mm/rev is significantly wider than that associated with feed = 0.25 mm/rev. This difference indicates that a selection of small feed

will cause a significant increase of the random tool motion. As discussed in Part 1, this range is determined by both the characteristics of microstructures in the material and the three cutting parameters of depth of cut, feed, and cutting speed. Therefore, a proper selection of the material processing to control the characteristics of microstructures in the material and a proper setting of the cutting parameters are two effective methods to limit the variance of the random excitation system for the vibration control of machining processes.

4 Parametric Tool Path Equations

Methods to perform suface topography analysis and construct the surface topograph of machined surfaces have been developed [8,9]. In this research, two parametric tool path equations are developed for the study of the surface topography. The two equations are built on spiral trajectory of the tool geometry and tool vibratory motion to determine the coordinates of the generated surface profiles in a three-dimensional space.

In the present work, the following two assumptions on the tool geometry are made for the development of the two equations.

1. The tool point is part of a circle having a radius R.
2. Both depth of cut and feed are held below some limiting values so that the roughness profiles produced during machining are solely made of a series of arc segments.

4.1 Equation to Determine Center Coordinates

Figures 5a and 5b present two roughness profiles along the feed direction taken from Figs. 1a and 1b, respectively. In Fig. 5a, all the intersection points between every pair of the nearby two circles are at a uniform distance, and the centers of all the circles are at the same height level in the direction of depth of cut. This profile represents a very special case indicating that the tool is stationary at its equilibrium position during machining.

In Fig. 5b, the centers of circles in the surface profile are not at the same height level due to the tool vibration with respect to its dynamic equilibrium position. The center

coordinate in the direction of depth of cut C_{jy}, where index j represents the j^{th} circle in the surface profile, can be determined from the system response $y(t)$ evaluated from Eq. (1). As indicated in Fig. 6, due to the presence of the tool lead angle, coordinate C_{jy} is related to the projection of the system response $y(t)$ in the direction of depth of cut [10]. This coordinate is given by

$$C_{jy} = Y(t) = y(t) * sinC_s \tag{9}$$

where $Y(t)$ = projection of the system response $y(t)$ in the direction of depth of cut, and

C_s = tool lead angle.

The center coordinate of the j^{th} circle in the feed direction C_{jx} is solely determined by the selected feed, and is independent of the tool vibratory motion. As shown in Fig. 5b, all the circles are at a uniform distance along the feed direction. Therefore, the following set of equations can be used to calculate the coordinates of centers in a given roughness profile.

$$\begin{aligned} C_{1x} &= \frac{2-1}{2} * (feed) \qquad C_{1y} = Y(t_i) \\ C_{2x} &= \frac{4-1}{2} * (feed) \qquad C_{2y} = Y(t_i + T) \\ &\cdots \\ C_{jx} &= \frac{2j-1}{2} * (feed) \qquad C_{jy} = Y[t_i + (j-1)T] \\ &\cdots \end{aligned} \tag{10}$$

where i = index for roughness profiles along the circumference or in the direction of cutting speed,

j = index for circles in a specified roughness profile,

t_i = time instant when the first circle in the specified roughness profile is generated,

T = time for one revolution of the workpiece during machining, and

$Y[t_i + (j-1) * T]$ = projection of the tool vibratory motion in the direction of depth of cut at the time instant $[t_i + (j-1) * T]$.

4.2 Equation to Determine Coordinates of Intersection Points

Note that the coordinates of the intersection points between a pair of the nearby two circles are neither at the same height nor at a uniform distance as a result of the tool vibration. The coordinates of these intersection points between the neighboring k^{th} and $(k+1)^{th}$ circles, denoted by the pair of (x_k, y_k), are governed by the solution of the following two simultaneous algebraic equations.

$$\begin{aligned} &(x_k - C_{kx})^2 + (y_k - C_{ky})^2 = R^2 \\ &(x_k - C_{(k+1)x})^2 + (y_k - C_{(k+1)y})^2 = R^2 \\ &for\ k = 1, 2, \cdots, (j-1) \end{aligned} \tag{11}$$

where R = tool nose radius.

A surface profile is uniquely determined when all the coordinates of the relevant centers and intersection points are known. Therefore, Eqs. (10) and (11) serve as the two basic parametric tool path equations to generate a roughness profile in two-dimensional space.

4.3 Consideration on the Third Dimension

Building on the two-dimensional roughness profile, a third dimension along the cutting speed direction or the direction of circumference of the workpiece should be added in order to complete the construction of surface topography. Essentially, adding the third dimension means to create a new two-dimensional roughness profile in the neighboring cross-section characterized by the time instant $(t_i + \Delta t)$ when the first radius in this neighboring cross-section is generated. As indicated in Figures 1a and 1b, the time lag Δt actually measures the distance between the first and the second cross-sections in the direction of circumference of the workpiece. The numerical value of the time lag Δt is equal to $\frac{T}{n}$ where n represents the number of the cross-sections the user intends to view within one cycle of the circumference. The parametric tool path equations used to generate a roughness profile in a cross-section characterized by the time lag of $m * \Delta t$ are identical to Eqs. (10) and (11) except that the

time instant t_i in Eq. (10) need to be replaced by the new time instant $(t_i + m * \Delta t)$ for m = 1,2, $\cdots$,n. Note that a two-dimensional roughness profile in a cross-section specified by the time instant $(t_i + n * \Delta t)$ can be directly obtained from the two-dimensional roughness profile in the cross-section specified by the time instant t_i after omitting the first circle in the profile, i.e., a "pushdown stack" relationship.

5 Simulation of Surface Topography

The process to simulate the topography of machined surfaces consists of computing the numerical values of the heights of a roughness profile along the feed direction in successive cross-sections taken along the workpiece circumference. The following five steps, as depicted in the simulation flow chart shown in Fig. 7, are used in the simulation process.

1. Simulation of the system response $y(t)$ for a given nominal chip load and a given random excitation system using the machining system model such as Eq. (1). Note that the other input function representing the residual chip load is automatically generated during the simulation process and then fedback to the input as indicated in Fig. 7 where the overlap factor μ has to be specified during the feedback process.

2. Scaling of the simulated system response $y(t)$ by a factor of $sinC_s$ where angle C_s is the tool lead angle.

3. Substitution of the scaled system response $Y(t)$ into the first parametric tool path equation, Eq. (10), to evaluate all the center coordinates in the surface profile. Equation (11) is used to evaluate the coordinates of all the intersection points between every pair of nearby two circles.

4. Computation of the coordinates of those points which are on the arc parts based on the geometric equation $(x^2 + y^2 = R^2)$.

5. Employment of a three-dimensional graphics package to plot the surface topography using the coordinate values obtained in Step 4.

Computer simulation for the construction of the surface topography of machined surfaces was carried out using the following parameters.

1. Boring bar diameter = 32 mm and its length = 170 mm.
2. Elastic modulus of the bar material = 210 x 10^9 N/m^2 and damping factor = 0.05.
3. Cutting stiffness = 1.80 x 10^6 N/m where workpiece material of SAE 1015 carbon steel is assumed.
4. Depth of cut = 0.50 mm and cutting speed = 95 m/min
5. Tool nose radius = 0.8 mm and the effective rake angle = 0^0.

Four different feed settings were used during the simulation process. Following the procedure discussed in Part 1 [1] and the calculated values of μ_a, σ_a^2, and $\rho(r)$ in Part 1 [1], the inputs related to the random excitation system, such as $\overline{\mu_s}$ and σ_s^2, are obtained as follows:

Case No	feed (mm/rev)	$\overline{\mu_s}\,(BHN)$	$\sigma_s^2\,(BHN^2)$	Meyer Exponent
Case 1:	0.10	126	172	0.454
Case 2:	0.15	126	170	0.454
Case 3:	0.20	126	169	0.454
Case 4:	0.25	126	166	0.454

The numerical computation process of the simulation can be found in [6]. The four surface topographies shown in Fig. 8 are plotted based on the databases obtained from the four simulation processes, respectively. The three dimensions used in Fig. 8 are the longitudinal direction representing the feed direction, the vertical direction representing the cutting speed direction, and the radial direction representing the direction along which the depth of cut is taken. Note that the textures of the four constructed surface topographies are

not deterministic. In fact, they are very similar to what have been routinely observed in practice.

6 Discussion of Results

6.1 Prediction of Roughness Indices

The four simulated surface topographies shown in Fig. 8 provide a qualitative visualization of the mechanism of surface irregularity generation during machining. They also offer a means to directly and quantitatively evaluate the roughness indices such as R_a, RMS, and Peak-to-Valley.

It is well known that taking a profile trace on an internal surface such as a bored hole involves a few technical concerns. The first concern could be the feasibility of carrying out such a measurement. For holes with a small diameter and a large ratio of length to diameter, taking a profile trace at the middle part of the entire length could be difficult. Secondly, there is no guarantee on the obtainable measuring accuracy. This not only requires the precision measuring instruments, but also needs skillful inspectors to do the job. Finally, the number of traces taken to assure the inspection quality may be critical since the measuring result varies from location to location on the machined surface.

In the present study, a surface roughness profile at a specified location can be constructed from the available numerical database. The R_a value of the roughness profile under consideration, without being measured on a surface profilometer, can be directly obtained based on the definition of of the R_a index (Roughness Average).

$$R_a = \frac{|y_1 - y_{average}| + |y_2 - y_{average}| + \cdots + |y_p - y_{average}|}{p} \tag{12}$$

where y_i = height coordinate of the i^{th} point on the profile,

$y_{average} = \frac{1}{p}(y_1 + y_2 + \cdots + y_p)$, and

p = number of points on the profile which are used in the calculation of $y_{average}$.

For an accurate R_a prediction, a number of roughness profiles should be used and an

average R_a should be calculated. The standard deviation of the R_a prediction, S_{Ra}, will indicate the accuracy of the R_a prediction. Table 2 lists the R_a values predicted from the simulation data used to construct the topographies for the four feed settings, together with the corresponding standard deviation values (S_{Ra}). An important observation is that the smaller the feed, the larger the standard deviation S_{Ra}. For example, $S_{Ra} = 0.838\ \mu m$ at feed $= 0.10\ mm/rev$ indicates a wide variation range from $1.198\ \mu m$ to $3.529\ \mu m$ for an individual R_a calculation. On the other hand, $S_{Ra} = 0.420\ \mu m$ at feed $= 0.25\ mm/rev$ indicates a rather small variation range from $3.088\ \mu m$ to $4.644\ \mu m$ for an individual R_a calculation. This important observation indicates that, with small feed values, an adequate amount of measurements should be taken to assess the surface topography. On the other hand, less measurements could be taken if a large feed was used to produce the machined surface.

6.2 Experimental Verification

To validate the present approach to study the mechanism of surface texture generation during machining, a comparison between the simulation and experimental results was made. Four boring machining tests were conducted on an experimental lathe. The cutting conditions used in the experiments were identical to those used in simulation as described in Section 5.

A TALYSURF-10 surface profilometer was used to collect surface profiles. A total of 20 surface profiles were collected from the four machined surfaces. In order to be consistent with the computer simulation work, skidless measurements were used. Figure 9 presents four typical profile traces obtained from the measurements. Table 3 lists the R_a values from the measurements as well as the R_a values from prediction along with their 90% confidence intervals based on the simulation data. As indicated in Table 3, nineteen out of the twenty R_a values associated with the measured surface profiles were within the confidence intervals based on the simulation, showing good agreements between the measured and predicted R_a

values.

Examining the measured data carefully, five R_a measurements were taken from an individual machined surface. The only measured profile for which the R_a value (4.0 μm) was outside the confidence interval [0.99, 3.91] was associated with the smallest among the four feed settings. This further suggests that more traces should be taken for a satisfactory quality inspection when small feeds are used.

6.3 Effects of Cutting Parameter Feed

There are three major effects of the cutting parameter feed on the dynamic generation of surface irregularities. The first effect is on the level of tool vibratory motion during machining. The smaller the feed, the larger the variance of the random excitation system. This random excitation system powerfully beats the cutting tool during machining. The second effect is that the smaller the feed, the larger the overlap factor μ of the regenerative mechanism [8], which effectively transmits the tool vibration from one revolution to its proceeding revolution. The third effect relates to the pattern recognition or the texture of machined surfaces. The profile pattern in the form of arc-chain can be easily observed when large feeds are used, such as shown in Fig. 8a (feed = 0.25 mm/rev, simulated) and in Fig. 9 (feed = 0.25 mm/rev, experimentally measured). Under such circumstances, the geometric-based theoretical formulas could be used to predict roughness indices such as R_a as a first approximation. However, this profile pattern in the form of arc-chain decays as the feed becomes small. For example, the arc-chain pattern can hardly be identified in Fig. 8d and Fig. 9 (feed = 0.1 mm/rev). In this situation, the geometrical-based formula can lead to a wrong assessment of surface topography.

There could be other effects of cutting parameter feed on the surface irregularity generation. The phenomenon of work hardening on the machined surface serves as one example. The overlapping phenomenon between two successive passes of the tool, which low feeds are responsible for, aggravates the degree of work hardening. This could also have an effect on

the cutting force variation.

7 Conclusions

1. A methodology to dynamically generate the topography of machined surfaces under various cutting conditions, workpiece materials, and tool geometries through computer simulation has been developed. The tool vibratory and geometrical motions are integrated to predict the surface texture formed during machining. The surface topographies simulated in the present work visualize the mechanism of surface irregularity generation.

2. A procedure has been developed to convert the random excitation system in terms of a normal distribution (unit of BHN) to an equivalent percentage variation in the nominal chip load (unit of mm^2) from the viewpoint of the cutting force generation. Such a conversion makes it possible to evaluate the instantanous cutting force during machining when subjected to random excitation.

3. The simulated surface topographies also confirm the conclusion derived in Part 1 of these two-part papers, i.e., the effect of tool vibration on the surface irregularity generation is quite significant at low values of feed due to the presence of a powerful random excitation system. In addition, the present work points out the importance of pattern recognition in the evaluation of surface roughness characteristics. The decaying of profile pattern in the form of arc-chain when a low value of feed is used suggests that the prediction of surface roughness indices based on geometrical-based theoretical formulas alone may not be accurate.

Acknowledgments

The authors acknowledge the support of the Systems Research Center at the University of Maryland at College Park under Engineering Research Centers Programs: NSFD CDF

8803012, and the support of the University of Illinois Office of Advanced Engineering Studies Research Program. Part of computer funds was provided by IBM Corporation.

References

1. G. M. Zhang and S. G. Kapoor, "Dynamic Generation of the Machined Surface, Part 1: Mathematical Description of the Random Tool Vibratory Motion," accompanied paper submitted to *Journal of Engineering for Industry* for review, February 1989.

2. H. E. Merrit, "Theory of Self-Excited Machine-Tool Chatter," *Journal of Engineering for Industry*, ASME Trans., Vol. 87, November 1965, pp. 447-454.

3. J. Tlusty, "Analysis of the State of Research in Cutting Dynamics," *Annals of the CIRP*, Vol. 27/2/1978, pp. 583-589.

4. W. L. Brogan, "Modern Control Theory," Quantum Publishers, Inc., 1974, p. 264.

5. S. G. Kapoor, G. M. Zhang, and L. L. Bahney, "Stability Analysis of the Boring Process System," *Proceedings of 12th NAMR Conference*, May 1984, pp. 454-459.

6. G. M. Zhang and S. G. Kapoor, "Dynamic Modeling and Analysis of the Boring Machining System," *Journal of Engineering for Industry*, Transactions of the ASME, Vol. 109, August 1987, pp. 219-226.

7. M. Kronenberg, "Machining Science and Application," Pergamon Press Inc., 1966, pp. 209-225.

8. D. J. Whitehouse, P. Vanherck, W. deBruin, C. A. vanLuttervelt, 'Assessment of Surface Typology Analysis Techniques in Turning,' *Annals of the CIRP*, Vol. 32/2, 1974, pp. 265-282.

9. T. S. Babin, J. W. Sutherland, and S. G. Kapoor, 'On the Geometry of End Milled Surfaces,' *Proceedings of 14th NAMR Conference*, May 1986, pp. 168-176.

10. G. M. Zhang, "Dynamic Modeling and Dynamic Analysis of the Boring Machining System," Ph.D. Thesis, University of Illinois at Urbana-Champaign, January 1986.

Table 1: Conversion Between Two Equivalent Representation Forms

Sample Order	Random Excitation System $\mu_a = 126, \sigma_{s1}^2 = 166$ (BHN)	Equivalent Percentage of Nominal Chip Load (P_i)	Random Excitation System $\mu_a = 126, \sigma_{s2}^2 = 172$ (BHN)	Equivalent Percentage of Nominal Chip Load (P_i)
1	119.0	-0.026	126.9	+0.003
2	118.0	-0.029	115.3	-0.039
3	123.3	-0.010	116.8	-0.034
4	137.8	+0.041	107.7	-0.069
5	145.8	+0.069	133.0	+0.025
6	141.1	+0.053	124.2	-0.007
7	120.1	-0.022	103.4	-0.086
8	126.3	+0.001	122.7	-0.012
9	150.0	+0.082	145.9	+0.069
10	103.0	-0.087	142.5	+0.057
11	113.2	-0.047	119.7	-0.023
12	142.3	+0.057	129.3	+0.012
13	127.6	+0.006	98.7	-0.105
14	116.6	-0.035	117.8	-0.030
15	114.5	-0.042	113.3	-0.047
16	127.3	+0.005	142.5	+0.057
17	120.4	-0.020	133.2	+0.026
18	134.0	+0.028	136.5	+0.037
19	111.4	-0.054	86.5	-0.157
20	123.0	-0.011	138.2	+0.043
21	127.9	+0.007	157.6	+0.107
22	123.7	-0.008	115.4	-0.039
23	116.4	-0.035	113.9	-0.045
24	142.8	-0.058	139.4	+0.047
25	124.0	-0.007	118.9	-0.026
26	106.0	-0.075	113.9	-0.045
27	129.1	+0.011	109.8	-0.061
28	133.0	+0.025	110.9	-0.056
29	122.1	-0.014	107.2	-0.071
30	149.6	+0.081	115.9	-0.037
31	140.6	+0.051	108.0	-0.068
32	129.0	+0.011	161.3	+0.119
33	124.3	-0.006	139.8	+0.048

Table 2: R_a Values Calculated from the Simulation Data for the Four Feeds

Feed (mm/rev)	0.10	0.15	0.20	0.25
1	2.587	2.677	2.811	3.234
2	1.995	2.207	2.544	3.168
3	1.614	1.825	2.206	3.915
4	1.484	1.752	2.146	3.838
5	2.257	2.275	2.371	3.984
6	1.521	1.679	2.036	3.782
7	1.903	1.967	2.284	3.955
8	1.903	1.961	2.324	3.088
9	2.522	2.520	2.729	3.313
10	1.198	1.527	2.080	3.947
11	2.104	2.147	2.545	3.330
12	3.332	3.389	3.555	3.978
13	3.339	3.365	3.550	4.009
14	2.638	2.554	2.600	3.259
15	3.307	3.214	3.235	3.701
16	3.529	3.542	3.616	4.050
17	4.466	4.336	4.339	4.646
18	2.340	2.318	2.527	3.107
$R_a = \frac{1}{18}[R_{a1} + \cdots + R_{a18}]$	2.447	2.514	2.750	3.350
Standard Deviation S_{Ra}	0.838	0.747	0.616	0.420
unit: μm				

Table 3: Comparison between the Measured and Simulated R_a Values

Simulation Results			Experimental Results (μm)					
Case No	Mean	90% C.I.	Profile 1	Profile 2	Profile 3	Profile 4	Profile 5	Average
1. f=0.10	2.45	[0.99, 3.91]	1.1	2.1	1.3	3.1	4.0	2.3
2. f=0.15	2.51	[1.21, 3.81]	1.4	2.8	2.9	3.2	3.7	2.8
3. f=0.20	2.75	[1.68, 3.82]	1.8	3.6	2.8	3.1	3.4	2.9
4. f=0.25	3.35	[2.62, 4.08]	3.0	2.7	3.8	3.2	3.3	3.2

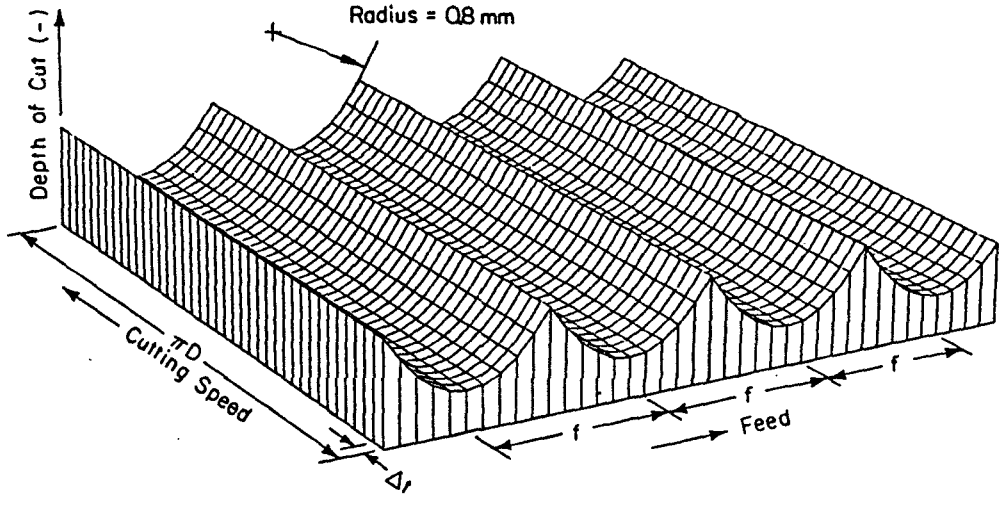

(a) Without Presence of Tool Vibration

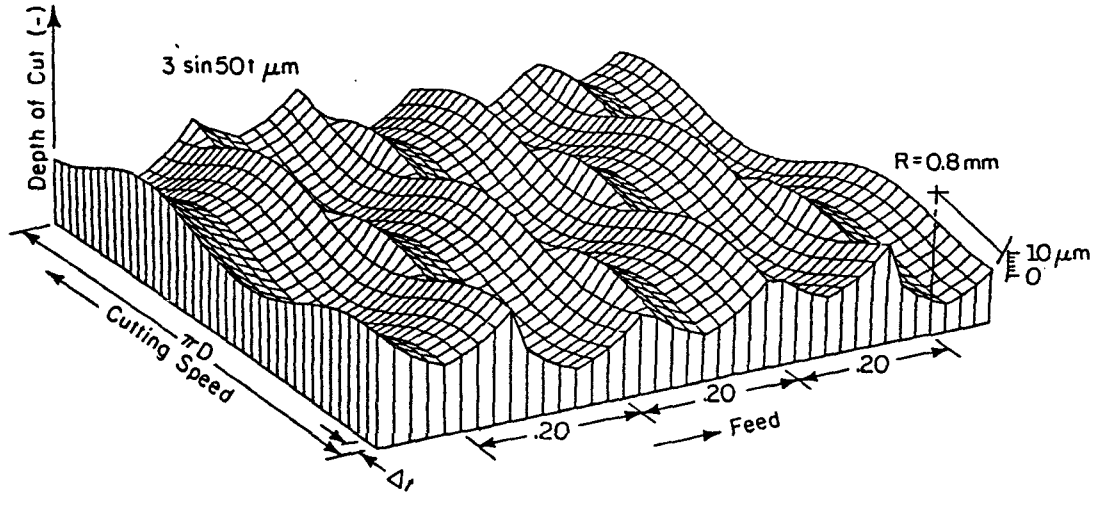

(b) Tool Vibration Motion 3 * sin 50 t (μm) Assumed

Fig. 1 Surface Topographies Assumed to Be Generated during Machining

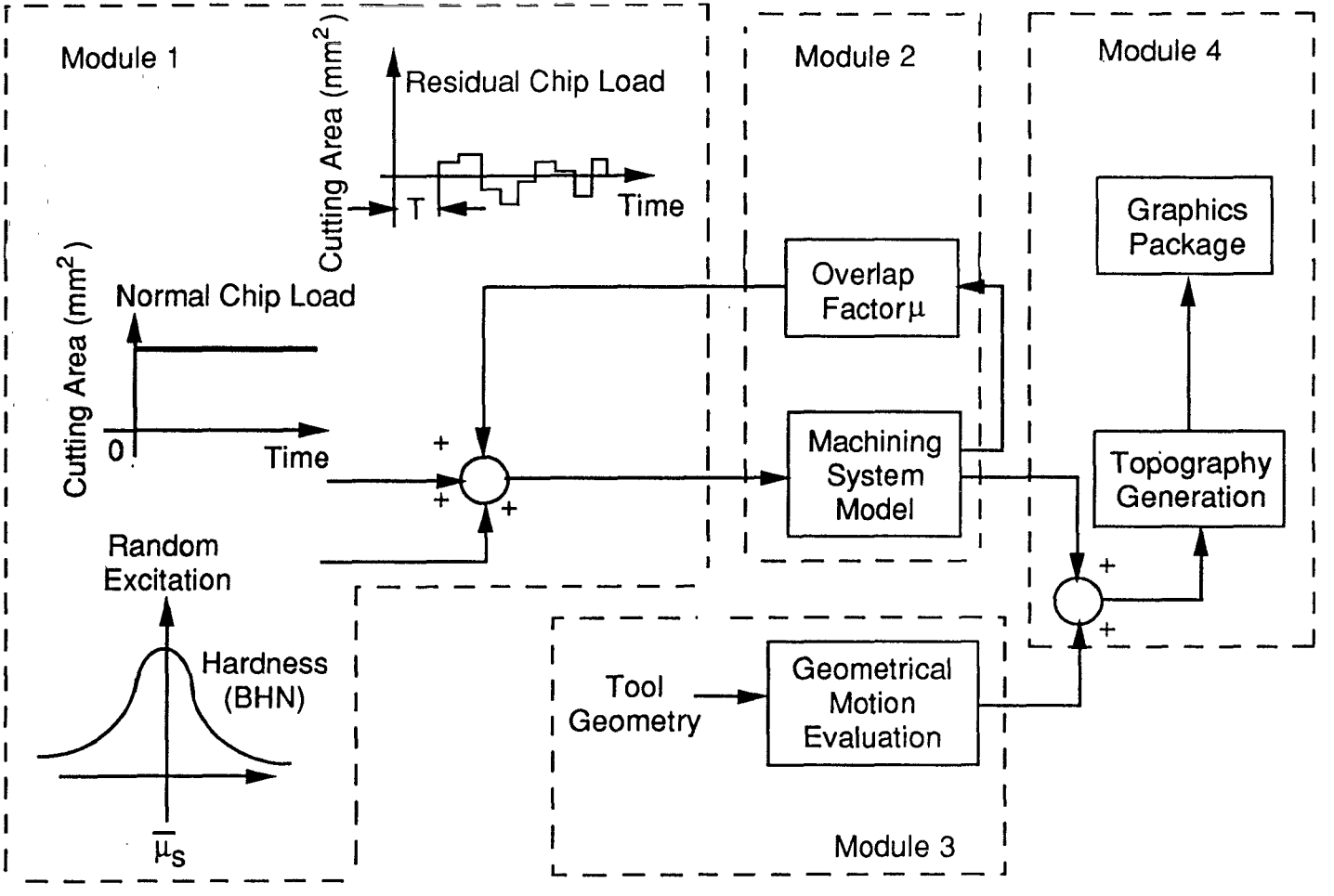

Fig. 2 Block Diagram Illustrating the Basic Methodology

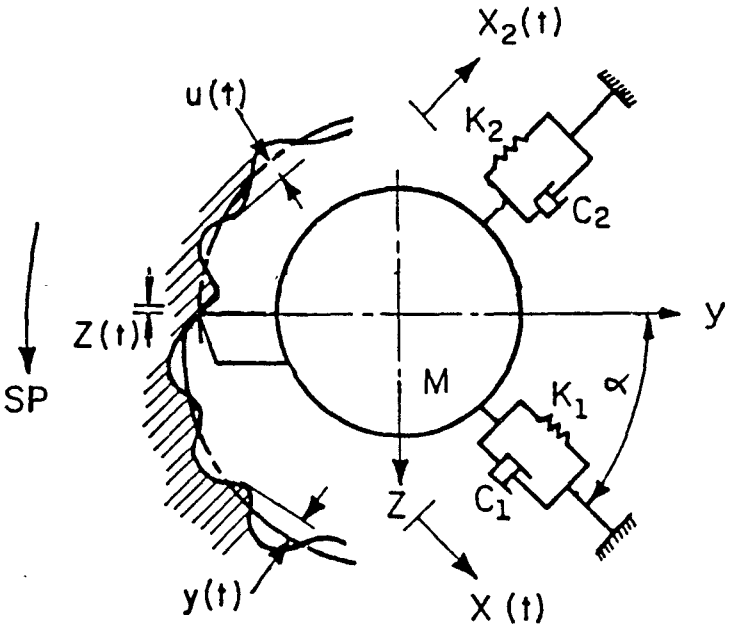

$K_1 = 4.07 \times 10^6$ N/M
$K_2 = 3.06 \times 10^6$ N/M
$C_1 = 104$ Kg/sec
$C_2 = 89.2$ Kg/sec
$\alpha = 80.0$ deg
M = 1.06 Kg

Fig. 3 Two-Degree-Of-Freedom Model

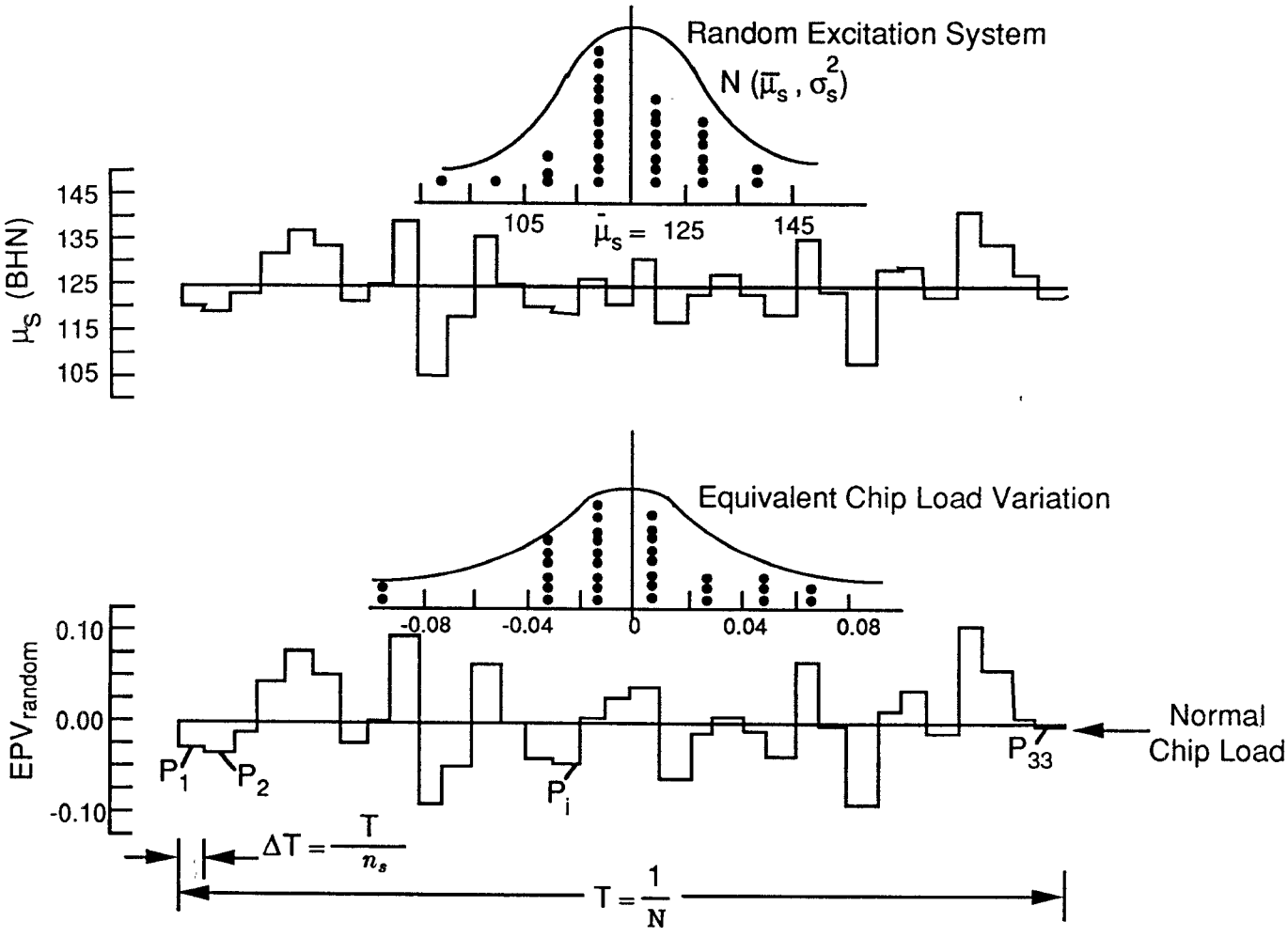

Fig. 4 Random Excitation System in Two Equivalent Forms

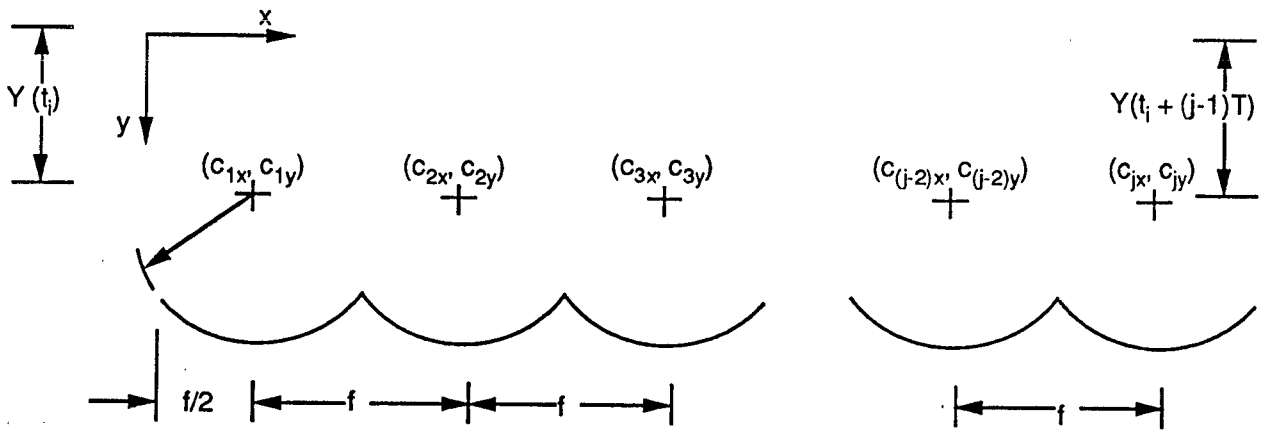

(a). Profile Without Presence of Tool Vibration

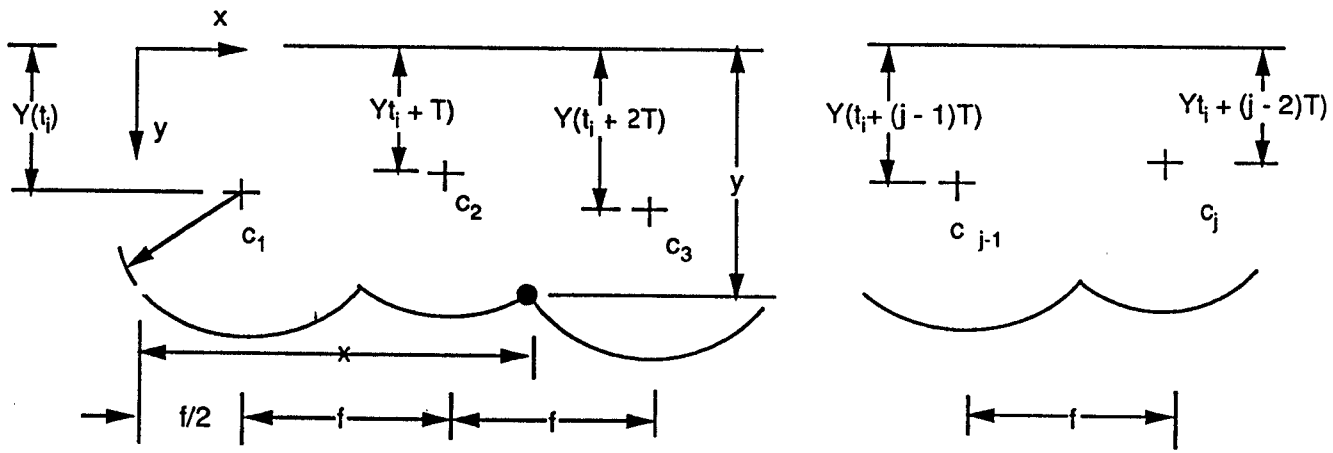

(b). Profile with Presence of Tool Vibration

Fig. 5 Derivation of Parametric Tool Path Equations

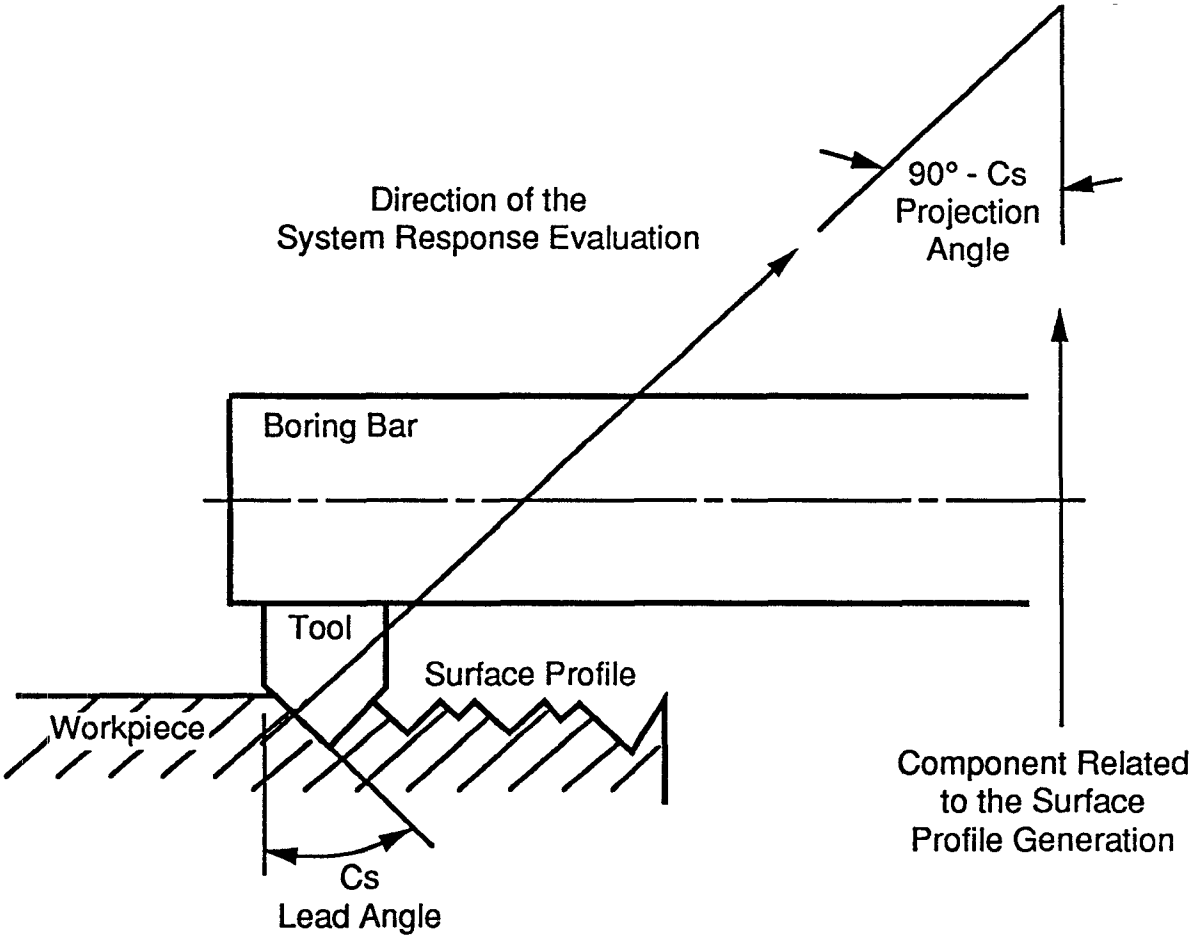

Fig. 6 Component of Tool Vibration for Surface Irregularity Generation

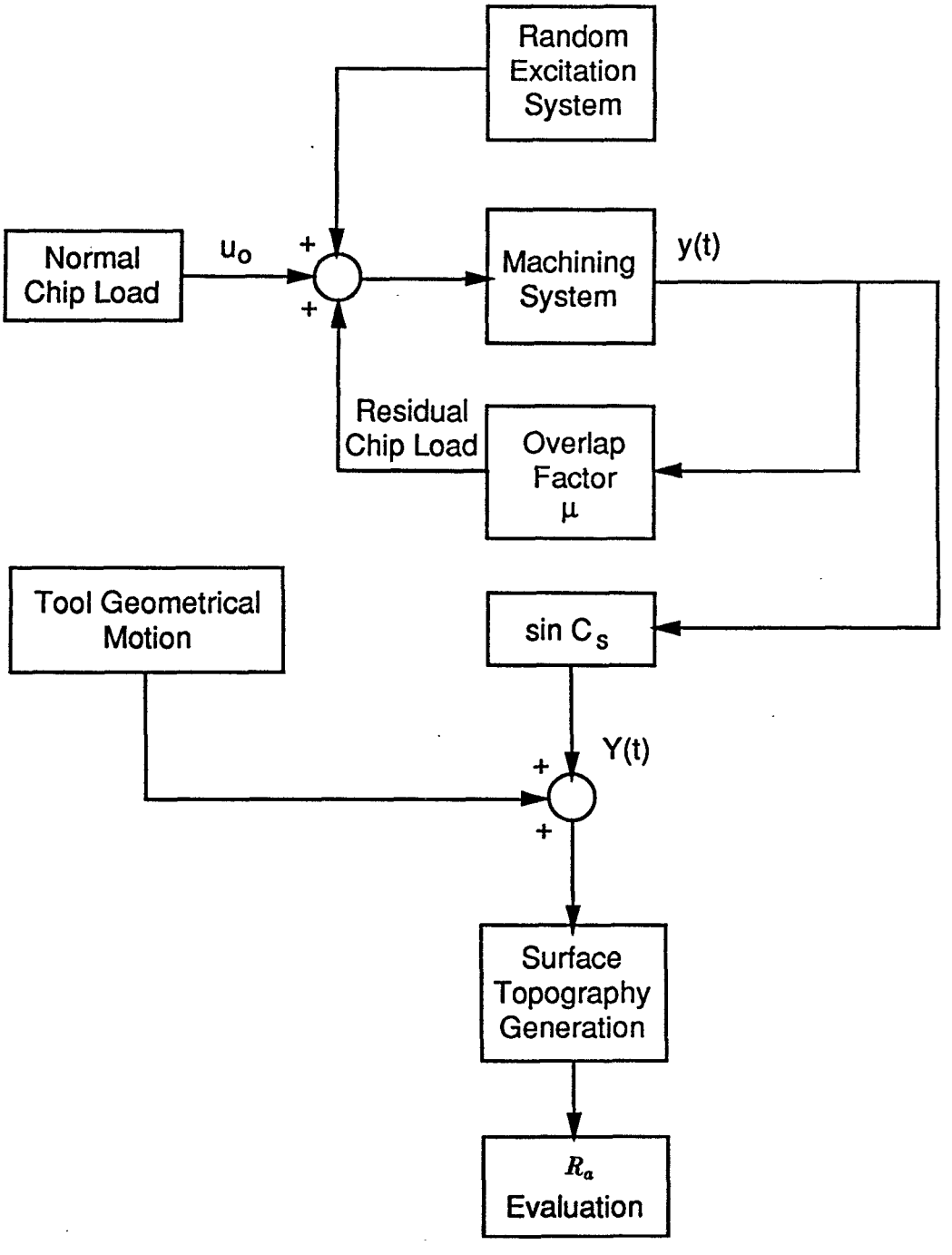

Fig. 7 Simulation Flow Chart

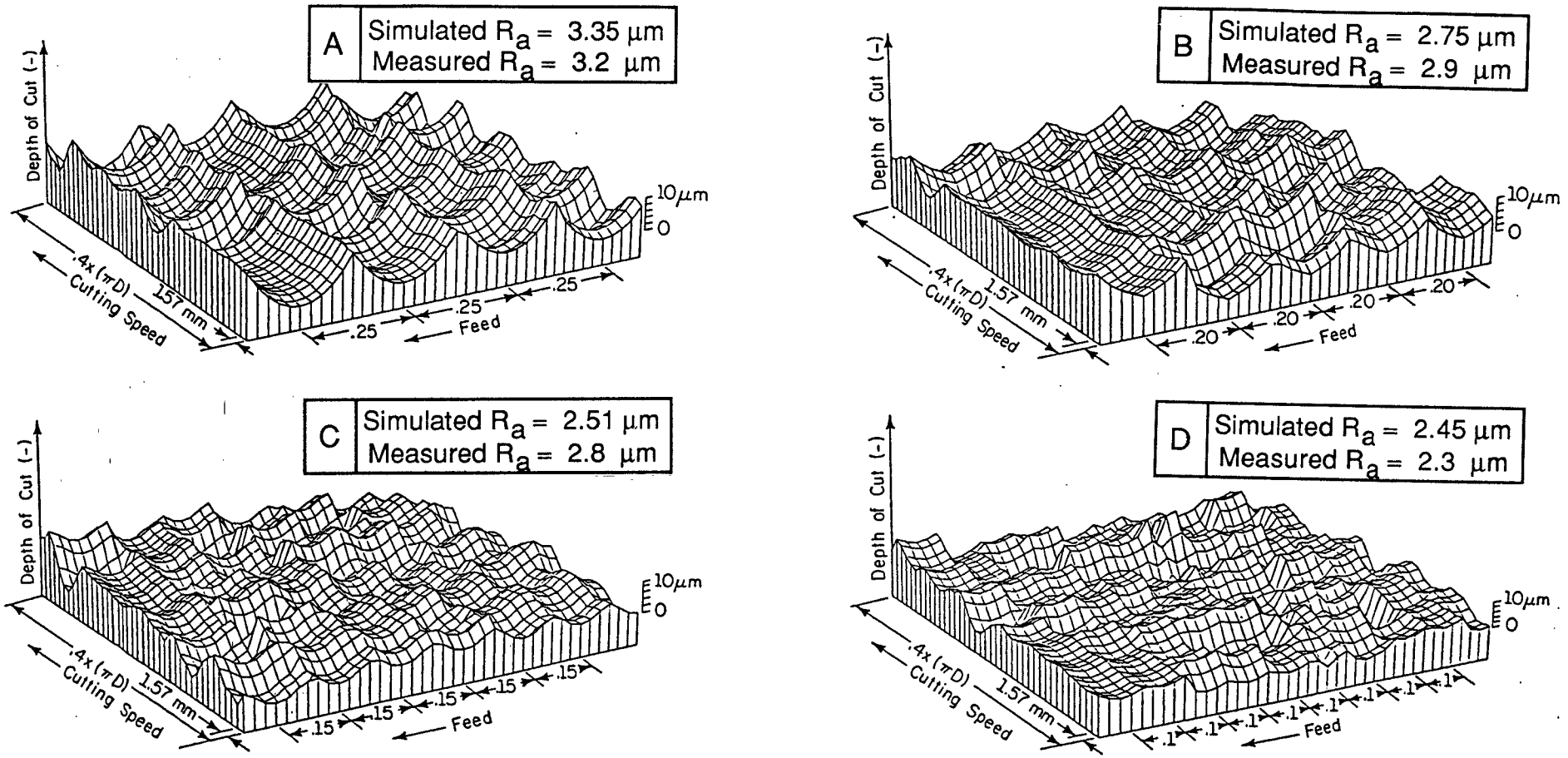

Fig. 8 Surface Topographies Generated under Four Cutting Conditions

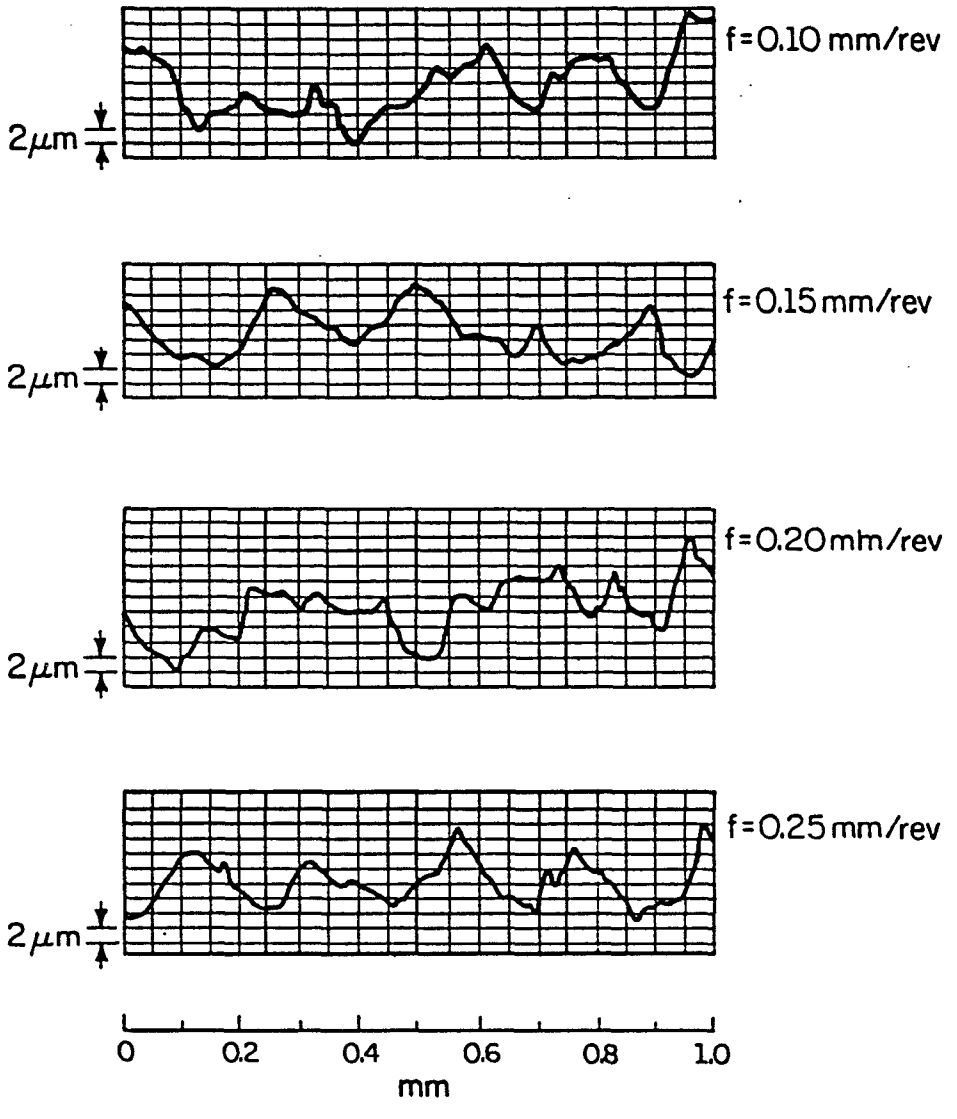

Fig. 9 Four Typical Traces Taken from the Four Machined Surfaces

NOMENCLATURE

A = system matrix of the system dynamic equations

R_a = surface roughness index, μm

A_i = magnitude of the random chip load variation at time $i * \Delta T$, mm^2

B = input matrix of the system dynamic equations

BHN = Brinell hardness number

C = output matrix of the system dynamic equations

C_{jx} = center coordinate in the direction of feed

C_{jy} = center coordinate in the direction of depth of cut

C_l = Chip load

C_s = lead angle of tool

d = depth of cut, mm

EPV_{random} = equivalent percentage variation

h_i = hardness value at i^{th} cutting location

$\overline{h}$ = mean hardness value of the material being machined

i = index for the order of samples taken along the circumference

j = index for the order of centers within a roughness profile

K_s = unit cutting force, N/mm^2

k = index for the order of intersection points within a roughness profile

l = number of total samples taken during the entire cutting process

m = meyer exponent in the cutting force evaluation

n_l = hardness mean location

n_s = number of samples taken along the circumference per one revolution

P_i = equivalent percentage of nominal chip load at time $i * \Delta t$

p = number of points taken on a roughness profile

P-to-V = surface roughness index, μm

RMS = surface roughness index, μm

ΔT = uniform time interval, sec

S_{Ra} = standard deviation of the R_a values evaluated from the simulation database, μm

N = spindle speed, rpm

$s(i * \Delta T)$ = unit step function with the jump discontinuity at time $(i * \Delta T)$

T = machining time during one revolution of workpiece, *sec*

x = coordinate of the k^{th} intersection point in the direction of feed

Y(t) = component of the system response in the direction of depth of cut, *mm*

y = coordinate of the k^{th} intersection point in the direction of depth of cut

y(t) = system response in the direction normal to the machined surface, *mm*

$y_{average}$ = mean of the profile heights, *mm*

μ = overlap factor of the regenerative process

μ_a = mean of the population distribution of hardness,
or mean of the sample hardness means, BHN

μ_s = sample hardness mean, BHN

$\overline{\mu_s}$ = mean of the sample hardness means, BHN

σ_s^2 = variance of the sample hardness means, BHN^2